



**HAL**  
open science

## **Synergistic antiarrhythmic effect of inward rectifier current inhibition and pulmonary vein isolation in a 3D computer model for atrial fibrillation**

Ali Gharaviri, Simone Pezzuto, Mark Potse, Giulio Conte, Stef Zeemering, Vladimír Sobota, Sander Verheule, Rolf Krause, Angelo Auricchio, Ulrich Schotten

### ► To cite this version:

Ali Gharaviri, Simone Pezzuto, Mark Potse, Giulio Conte, Stef Zeemering, et al.. Synergistic antiarrhythmic effect of inward rectifier current inhibition and pulmonary vein isolation in a 3D computer model for atrial fibrillation. EP-Europace, 2021, 23 (Supplement\_1), pp.i161-i168. 10.1093/europace/euaa413. hal-03452233

**HAL Id: hal-03452233**

**<https://inria.hal.science/hal-03452233>**

Submitted on 26 Nov 2021

**HAL** is a multi-disciplinary open access archive for the deposit and dissemination of scientific research documents, whether they are published or not. The documents may come from teaching and research institutions in France or abroad, or from public or private research centers.

L'archive ouverte pluridisciplinaire **HAL**, est destinée au dépôt et à la diffusion de documents scientifiques de niveau recherche, publiés ou non, émanant des établissements d'enseignement et de recherche français ou étrangers, des laboratoires publics ou privés.

1 **Synergistic antiarrhythmic effect of inward rectifier current**  
2 **inhibition and pulmonary vein isolation in a 3D computer model**  
3 **for atrial fibrillation**

4 Ali Gharaviri, PhD<sup>a</sup>, Simone Pezzuto<sup>a</sup>, PhD, Mark Potse, PhD<sup>b,c,d</sup>, Giulio Conte, MD, PhD<sup>a,e</sup>,  
5 Stef Zeemering, PhD<sup>f</sup>, Vladimír Sobota, MSc<sup>f</sup>, Sander Verheule, PhD<sup>f</sup>, Rolf Krause, PhD<sup>a</sup>,  
6 Angelo Auricchio, MD, PhD<sup>a,e</sup>, Ulrich Schotten, MD, PhD<sup>f</sup>

7 a: Center for Computational Medicine in Cardiology, Institute of Computational Science,  
8 Università della Svizzera italiana, Lugano, Switzerland.

9 b: Carmen team, Inria Bordeaux – Sud-Ouest, Talence, France.

10 c: Université de Bordeaux, IMB, UMR 5251, F-33400 Talence, France.

11 d: IHU Liryc, Electrophysiology and Heart Modeling Institute, foundation Bordeaux  
12 Université, Bordeaux, France.

13 e: Fondazione Cardiocentro Ticino, Lugano, Switzerland.

14 f: Department of Physiology, Maastricht University, Maastricht, The Netherlands.

15  
16 **Corresponding author:**

17 Angelo Auricchio, MD PhD  
18 Division of Cardiology,  
19 Fondazione Cardiocentro Ticino  
20 Via Tesserete 48  
21 6900 Lugano, Switzerland  
22 Tel.: +41 91 805 33 40  
23 E-Mail: [angelo.auricchio@cardiocentro.org](mailto:angelo.auricchio@cardiocentro.org)  
24

25 Number of words (excluding references, table, and figures): 3625

27 **Abstract**

28 **Aims:** Recent clinical studies showed that antiarrhythmic drug (AAD) treatment and  
29 pulmonary vein isolation (PVI) synergistically reduce atrial fibrillation (AF) recurrences after  
30 initially successful ablation. Among newly developed atrial-selective AADs, inhibitors of the  
31 G-protein-gated acetylcholine-activated inward rectifier current ( $I_{K_{ACh}}$ ) were shown to  
32 effectively suppress AF in an experimental model but have not yet been evaluated clinically.  
33 We tested *in-silico* whether inhibition of inward rectifier current or its combination with PVI  
34 reduces AF inducibility.

35 **Methods:** We simulated the effect of inward rectifier current blockade ( $I_K$  blockade), PVI,  
36 and their combination on AF inducibility in a detailed 3-dimensional model of the human  
37 atria with different degrees of fibrosis.  $I_K$  blockade was simulated with a 30% reduction of its  
38 conductivity. AF was initiated using incremental pacing applied at 20 different locations, in  
39 both atria.

40 **Results:**  $I_K$  blockade effectively prevented AF induction in simulations without fibrosis as  
41 did PVI in simulations without fibrosis and with moderate fibrosis. Both interventions lost  
42 their efficacy in severe fibrosis. The combination of  $I_K$  blockade and PVI prevented AF in  
43 simulations without fibrosis, with moderate fibrosis, and even with severe fibrosis. The  
44 combined therapy strongly decreased the number of fibrillation waves, due to a synergistic  
45 reduction of wavefront generation rate while the wavefront lifespan remained unchanged.

46 **Conclusions:** Newly developed blockers of atrial specific inward rectifier currents, such as  
47  $I_{K_{ACh}}$ , might prevent AF occurrences and when combined with PVI effectively suppress AF  
48 recurrences in human.

49 **Keywords:** Antiarrhythmic drug, Inward rectifier currents, Catheter ablation, Atrial  
50 Fibrillation recurrence, *In-silico* study.

52 **What's new**

- 53 • We simulated the efficacy of inward rectifier current blockade and its combination  
54 with PVI on prevention of AF initiation in different degrees of atrial fibrosis.
- 55 • The combination of inward rectifier blockade with PVI synergistically reduced the  
56 likelihood of AF initiation in simulations with severe atrial fibrosis.
- 57 • The inward rectifier current blockade adjunctive to PVI strongly reduced the number  
58 of fibrillation waves and new wavefront generation rate, while increasing the wave  
59 size, and thereby strongly prevented AF induction.

60 **Condensed Abstract**

61 Continuation of antiarrhythmic drugs after catheter ablation has been shown to reduces AF  
62 recurrences. We studied whether inhibition of inward rectifier current combined with catheter  
63 ablation reduces AF inducibility in a realistic 3D computer model of human atria. We showed  
64 that either inward rectifier current inhibition or PVI separately cannot significantly reduce AF  
65 initiation likelihood in the simulations with severe atrial fibrosis, while their combination  
66 can.

67

68

## 69 **1 Introduction**

70 Despite the development of pharmacological therapies for patients with atrial fibrillation  
71 (AF), a large proportion of AF patients are not arrhythmia-free.<sup>1</sup> Pharmacological therapy is  
72 less effective in non-paroxysmal AF patients than in paroxysmal AF patients, indicating the  
73 significance of structural remodelling in the efficacy of pharmacological therapy. If the  
74 treatment with antiarrhythmic drugs (AAD) fails, patients receive catheter ablation (CA) as a  
75 second-line treatment.<sup>2</sup> CA is also associated with a rather disappointing long term outcome,  
76 as after one year AF reoccurs in up to 30% of patients after PVI, despite proven complete PV  
77 isolation supporting the presence of driver mechanisms of AF located outside the PV area.<sup>3,4</sup>  
78 The recent EAST trial stresses the need for early and effective rhythm control strategies<sup>5</sup> and  
79 combination of AADs with CA may be a strategy to achieve this. In a recent study,  
80 Duytschaever et al. demonstrated that continuing previously ineffective treatment with AAD  
81 after CA is associated with lower prevalence of atrial tachyarrhythmias after one year.<sup>6</sup>  
82 However, the mechanisms underlying this synergistic inhibition of AF recurrences is not well  
83 understood. Also, current AADs having potential side effects such as ventricular pro-  
84 arrhythmia. For these reasons, atrial-selective AADs that do not affect ventricular conduction  
85 or repolarization have been developed. Examples are blockers of the ultra-rapid inward  
86 rectifier current ( $I_{Kur}$ ), small-conductance  $Ca^{2+}$ -activated  $K^{+}$ -currents (SK), and the G-protein-  
87 gated acetylcholine-activated inward rectifier current ( $I_{KAch}$ ). A blocker of  $I_{KAch}$  (XAF-1407)  
88 has recently been demonstrated to effectively suppress AF in an experimental equine model.<sup>7</sup>  
89 Here, we tested whether inward rectifier current blockade reduces AF inducibility and  
90 whether the combination of inward rectifier blockade with PVI prevents AF recurrences in a  
91 computer model of human atria.

## 92 **2 Methods**

### 93 **2.1 Computational model of AF**

94 Computer simulations were performed on a highly detailed 3D model of human atria.<sup>8</sup> The  
95 model geometry was based on magnetic resonance imaging data of a subject with normal  
96 atria with manually added anatomical structures and properties such as three layers of fibre  
97 orientations, endocardial trabeculated network, Bachmann's bundle, wall thickness  
98 heterogeneities, and left atrial appendage trabeculated network.<sup>8</sup> Several studies have shown  
99 that these structures have an essential role in AF initiation and maintenance.<sup>9,10</sup> The model  
100 consisted of approximately 5 million nodes spaced at 200 $\mu$ m.  
101 Action potential propagation was simulated with a monodomain reaction-diffusion equation  
102 using the Courtemanche-Ramirez-Nattel atrial cell model.<sup>11</sup> AF-induced changes in ionic  
103 currents were incorporated by setting the conductivities for  $I_{to}$ ,  $I_{Ca,L}$ , and  $I_{K1}$  at 40%, 35%, and  
104 200% of their normal values, respectively.<sup>12</sup> Simulations were performed using the propag-5  
105 software<sup>13</sup> and run on a Cray XC50 supercomputer with GPU support.

### 106 **2.2 Modelling of inward rectifier current blockade**

107 The inward rectifier background current ( $I_{K1}$ ) and the G-protein-gated acetylcholine-activated  
108 inward rectifier current ( $I_{KAch}$ ) show identical current-voltage relationships and are, therefore,  
109 indistinguishable on the single cell level.<sup>14</sup> Thus, both currents are adequately represented by  
110 one total inward rectifier conductance in computer models. For this reason, inhibition of  $I_{KAch}$   
111 was simulated by reduction of this total inward rectifier current. The conductance of the  
112 current was reduced by 30% resulting in a prolongation of the atrial action potential duration  
113 by approximately 20ms, which is in the range of experimental studies.<sup>15,16</sup>

## 114 **2.3 Distribution of tissue fibrosis**

115 The effect of structural remodelling was simulated by different degrees of fibrosis. The  
116 conditions without, with moderate, and with severe fibrosis were modelled by setting 0%,  
117 50%, and 70% of the elements in the model as fibrotic, respectively. Fibrotic elements  
118 remained conductive along the fibre direction and isolated in the two transverse directions.  
119 This modelling of atrial tissue fibrosis agrees with the experimental study by Spach et al. that  
120 revealed loss of side-to-side electrical connections between atrial muscle bundles in fibrotic  
121 atrial tissue.<sup>17</sup> The fibrosis was distributed within the subepicardial layer, while the atrial  
122 bundles remained intact. The spatial distribution of fibrosis was uneven, with patches or  
123 island presenting higher degree of fibrosis. Such distribution was based on spatially  
124 correlated, anatomy-tailored random fields.<sup>8, 18</sup>

## 125 **2.4 Modelling of Pulmonary vein isolation**

126 In PVI simulations, two antral circumferential lines isolated the PV from the atria. Virtual  
127 ablation lesions consisted of tissue volumes modelled by non-conductive elements.

## 128 **2.5 AF initiation in pre- and post-catheter ablations**

129 AF initiation likelihood was assessed by applying incremental pacing at 20 different locations  
130 in both atria and compared between the control (no inward rectifier current inhibition and no  
131 CA), inward rectifier current blockade ( $I_K$  blockade), PVI, and  $I_K$  blockade + PVI groups.  
132 Pacing locations were selected based on reported possible sources of extra-PV ectopic focal  
133 activity in AF patients, including the area between the PVs, left atrium, left atrial appendage,  
134 right atrial appendage, coronary sinus, superior caval vein, inferior caval vein, and right  
135 atrium.<sup>19</sup> All pacing sites were located outside the ablated area. In each simulation, AF was  
136 initiated by applying incremental pacing with a duration of 2 seconds at a selected pacing

137 site. In total, 14 stimuli were applied with the pacing cycle length gradually reducing from  
138 280ms to 124ms. After the pacing period, the simulations were continued for another 3  
139 seconds with no pacing.

## 140 **2.6 Definition of successful AF initiation**

141 The stimulation protocol outcome was analysed in terms of the type of self-sustained rhythm  
142 after 2 seconds of stimulation. If no activation after pacing was noted, the initiation was  
143 considered unsuccessful. Otherwise, a distinction between AF and atrial flutter (AFL) was  
144 made, with the latter not being considered as successful AF initiation. AF and AFL  
145 conduction patterns were differentiated by analysing the reconstructed 12-lead ECGs, as  
146 described in detail in the supplementary material.

## 147 **2.7 Detection and tracking of fibrillation waves**

148 A fibrillation wave was defined as a contiguous volume in which all nodes had  
149 transmembrane voltage above  $-60$  mV. Wave size was defined as the number of model  
150 elements within this contiguous volume. Both the number of waves and wave sizes were  
151 calculated at each millisecond of simulated time.

152 Fibrillation waves were tracked in both time and space, as described in our previous study.<sup>20</sup>

153 Briefly, the temporal dynamics of waves can be described by three events:

- 154 • Generation: appearance of a new wave either due to wave break or transmural  
155 conduction.
- 156 • Fusion: the merge of two or more waves into one wave.
- 157 • Extinction: the extinction of a wave, due to encountering either a boundary or  
158 unexcitable tissue.

## 159 **2.8 Statistics**

160 All statistical analyses were performed using GraphPad Prism software version 8.0. The  
161 values are expressed as means  $\pm$  SD. Statistical tests were performed to compare the effect of  
162 three parameters (fibrosis levels,  $I_K$  blockade, and PVI) in AF initiation rate, using two-way  
163 ANOVA followed by post hoc Bonferroni test. A value of  $P < 0.05$  was considered to be  
164 significant.

165

## 166 **3 Results**

167 In total, 240 simulations were performed. The simulations consisted of 4 groups: control (no  
168 interventions), inward rectifier current blockade ( $I_K$  blockade), PVI, and the combination of  
169 inward rectifier current blockade and PVI ( $I_K$  blockade + PVI). Twenty simulations were  
170 performed for each degree of fibrosis, resulting in the total of 60 simulations performed in  
171 each group.

### 172 **3.1 AF initiation**

173 Figure 1A displays several action potentials recorded during simulated AF episodes in the  
174 control and  $I_K$  blockade simulations.  $I_K$  inhibition caused prolongation of action potential  
175 duration at 90% of repolarization ( $APD_{90}$ ) from  $119 \pm 12.5$ ms in control to  $136 \pm 10.4$ ms.

176 Figure 2 depicts representative conduction patterns and corresponding ECG leads of  $I_K$   
177 blockade, PVI, and  $I_K$  blockade + PVI simulations under the condition of severe fibrosis. As  
178 depicted in this figure, both  $I_K$  blockade and PVI failed to prevent AF initiation in severe  
179 fibrosis simulations, while the combination rendered the atria uninducible.

180 Figure 3 shows initiation rates of atrial tachycardia in all simulation groups in the presence of  
181 different degrees of fibrosis. The figure shows that in the absence of fibrosis,  $I_K$  blockade

182 caused a significant reduction in AF initiation likelihood when compared to control, either by  
183 preventing initiation of AF or by transforming initiated AF into AFL.  $I_K$  blockade failed to  
184 significantly reduce AF initiation rate in the simulations with moderate or severe fibrosis. In  
185 PVI simulations, we observed significant reduction in AF initiation likelihood in the absence  
186 or in the presence of moderate fibrosis when compared to control, while no significant  
187 reduction was noted in the simulations with severe fibrosis. In the simulations that combined  
188 PVI with  $I_K$  blockade, we observed a comparable reduction in AF initiation likelihood as in  
189 PVI simulations in the absence of fibrosis or in the presence of moderate fibrosis. The  
190 combination of  $I_K$  blockade and PVI further reduced AF initiation likelihood by at least half  
191 in the simulations with severe fibrosis.

### 192 **3.2 Fibrillation pattern complexity**

193 Overall, a significant increase in AF cycle length was observed in all simulation groups when  
194 compared to control, regardless of the fibrosis degree, as shown in Table 1. When compared  
195 to control, no significant differences in the excitable gap were detected in any simulation  
196 group (see Table. 1).

197 Examples of wave lifespans in control,  $I_K$  blockade, PVI, and PVI accompanied with  $I_K$   
198 blockade simulations with severe fibrosis are illustrated in figure 4A. An increase in the  
199 fibrosis degree in control simulations led to a significant increase in fibrillation wave  
200 generation rate, quantified as the slope of the fitted line to the wave lifespans, and therefore a  
201 significant increase in AF conduction pattern complexity, quantified as the average number  
202 of waves per cycle (Figure 4B & C). The increase in conduction pattern complexity was due  
203 to the reduction of wave size and higher rate of new wavefront generation, while wavefront  
204 lifespan medians remained unchanged (Figure 4D & E). In the simulations without fibrosis,  
205  $I_K$  blockade caused a significant reduction in the average number of waves per cycle, by

206 increasing the wave sizes and significantly reducing the rate of wavefront generation.  
207 However, this effect of  $I_K$  blockade disappeared in the simulations with moderate and severe  
208 fibrosis. PVI significantly reduced new wavefront generation rate in the simulations without  
209 fibrosis as well as in the simulations with moderate fibrosis. Nevertheless, this effect faded in  
210 PVI simulations with severe fibrosis. In  $I_K$  blockade combined with PVI simulations, the  
211 synergistic interaction between the wave size enlargement caused by  $I_K$  blockade and the  
212 reduction in atrial tissue mass caused by PVI further reduced the available space for  
213 wavefront interactions. This resulted in significantly decreased rate of new wavefront  
214 generation, and therefore in a smaller number of fibrillation waves.

215

## 216 **4. Discussion**

217 We investigated the isolated and combined effects of inward rectifier current blockade and  
218 PVI on AF initiation in the presence of various degrees of atrial fibrosis. Both inward  
219 rectifier blockade and PVI effectively reduced the rate of AF induction at low degrees of  
220 atrial fibrosis but lost their efficacy in severely fibrotic atria. In the simulations with severe  
221 fibrosis the combination of inward rectifier blockade and PVI effectively suppressed AF  
222 recurrences, while either of the interventions was not efficient individually. The synergy  
223 between both interventions resulted in reduction in the number of fibrillation waves. The  
224 main underlying mechanism behind this effect was a reduction in the rate of new wavefront  
225 generation, leaving the lifespan of fibrillation waves unaffected.

### 226 **4.1 Effect of inward rectifier current blockade and PVI in previous in-silico studies**

227 So far, several *in-silico* studies investigated the effect of different antiarrhythmic drugs  
228 (single-channel or multiple-channel block) or CAs on AF initiation, perpetuation and  
229 termination.<sup>21, 22</sup>

230 Among the large variety of potassium channels expressed in human atria, the inward rectifier  
231 currents  $I_{K1}$  and  $I_{KAch}$  play a significant role in AF perpetuation. Heterogeneous shortening of  
232 the atrial effective refractory period caused by vagally modulated  $I_{KAch}$  channels are thought  
233 to be the mechanism underlying vagally-induced AF.<sup>23</sup> Hence, inhibition of  $I_{KAch}$  may  
234 minimize the effect of  $I_{KAch}$  modulations and could be a future therapeutic option for vagally-  
235 induced AF.<sup>23</sup> Dobrev and colleagues have demonstrated that an increase of constitutively  
236 active  $I_{KAch}$  strongly contributes to atrial action potential shortening in human persistent AF.<sup>14</sup>  
237 Also  $I_{KAch}$  is active in atrial but not in ventricular cells so that inhibition of  $I_{KAch}$  is not  
238 expected to prolong ventricular action potential. For these reasons inward rectifier currents  
239 are an attractive target for antiarrhythmic treatment of AF.<sup>22, 24</sup> Importantly,  $I_{K1}$  and  $I_{KAch}$  only  
240 differ in their single channel conductance but their single cell level current-voltage  
241 relationships are identical.<sup>14</sup> Thus, both currents are adequately represented by the total  
242 inward rectifier conductance in computer models.

243 The influence of inward rectifier current inhibition on AF initiation, termination, and  
244 conduction pattern was investigated in several computational studies.<sup>21, 22</sup> Sánchez et al.  
245 demonstrated that inward rectifier inhibition led to higher arrhythmia organization by  
246 enlarging wave sizes, increasing wave meandering, and reducing the number of secondary  
247 wavelets.<sup>24</sup> These findings are in line with our results of inward rectifier current inhibition in  
248 the atria without fibrosis in the present study. However, we observed significant efficacy loss  
249 of inward rectifier current blockade in reducing the number of fibrillation waves and AF  
250 termination or initiation in the presence of moderate or severe fibrosis.

251 The effectiveness of PVI to terminate AF in representative virtual atria was assessed in  
252 several studies.<sup>25</sup> Recent proof-of-concept in-silico studies investigated the role of atrial  
253 fibrosis in ablation failure using detailed patient-specific image-based models.<sup>26</sup> These  
254 studies demonstrated that both the patient-specific degree and the distribution of fibrosis are a

255 determining factor in AF initiation and maintenance.<sup>27</sup> McDowell et al. demonstrated that  
256 modelling of ablation lesions in the persistent rotor core meandering regions renders AF  
257 uninducible.<sup>27</sup> Here, we simulated the combination of PVI and inward rectifier current  
258 blockade and studied the mechanisms underlying the synergy between these two treatment  
259 options on prevention of AF initiation.

#### 260 **4.2 Synergism between inward rectifier inhibition and PVI to prevent AF recurrence**

261 The development of efficient therapy against AF remains an important unfulfilled clinical  
262 need. Treatment with AADs has been considered as the first-line therapy<sup>2</sup> and recently has  
263 been demonstrated to reduce major cardiovascular adverse events in patients with AF.<sup>5</sup>  
264 However, the efficacy of AADs decreases with AF progression.<sup>2</sup> CA has been recognized as  
265 an alternative therapeutic modality in AF treatment, which has been highlighted in several  
266 studies to be more efficient than AAD therapy to prevent AF recurrences.<sup>21</sup> Nevertheless, CA  
267 results remain suboptimal, particularly in non-paroxysmal AF patients.<sup>28</sup> Recently, there has  
268 been a growing interest in the effect of AAD continuation after CA.<sup>6</sup> As reported in the  
269 POWDER-AF trial, the AADs, despite being inefficient before ablation, are becoming  
270 efficient in reducing AF recurrence after CA.<sup>6</sup> The mechanisms underlying this synergy  
271 between AADs and CA in AF recurrence prevention were so far not well understood.  
272 Our simulations showed that either inward rectifier current inhibition alone or PVI alone can  
273 significantly prevent initiation of AF only in the presence of no or moderate fibrosis, while  
274 both became inefficient in the presence of severe fibrosis. When both strategies were  
275 combined, little contribution to further reduction of AF inducibility in the simulations with no  
276 or moderate fibrosis was observed. In severe fibrosis, inward rectifier blockade in  
277 combination with PVI strongly reduced the number of fibrillation waves, increased their size  
278 and strongly prevented successful AF induction. This effect was associated with significant

279 decline in the rate of new wave generation while wavefront lifespan remained unaltered. The  
280 observed synergism might be explained by the fact that both PVI as well as the wavelength  
281 prolongation by the inward rectifier blockade restrict the available space for wave-front-  
282 wave-tail interactions which reduces the likelihood for wave break and generation of new  
283 waves. Our results indicate that the newly developed inhibitors of  $I_{K_{ACh}}$  have a potential to  
284 show the observed synergism with PVI to prevent AF induction in a clinical setting.

## 355 **5 Limitations**

356 Inter-individual variabilities in anatomy, atrial size, fibre orientation, and wall thickness were  
357 not considered in our study. Several clinical and simulation studies reported the effect of  
358 variability in atrial geometry and the pattern of fibrosis on initiation of fibrillatory waves.<sup>26,</sup>  
359 <sup>29-31</sup> Studying the effect of variations in the pattern of atrial fibrosis on AF inducibility is  
360 certainly warranted. Although based on clinical data, the pattern of atrial fibrosis was  
361 generated algorithmically in this study. We investigated the effect of inward rectifier current  
362 inhibition, whereas several other currents have been shown to play an important role in AF  
363 termination. Moreover, we did not investigate inhibition of multiple ion channels on AF  
364 dynamics. Finally, heterogeneity in ionic parameters in our model has not been implemented  
365 on purpose in order to avoid confounding factors.

## 366 **6 Conclusion**

367 This study shows that adding inward rectifier current inhibition to PVI caused a significant  
368 reduction in AF recurrences even in the atria with severe fibrosis, whereas both treatments  
369 alone failed to prevent AF initiation in severely fibrotic atria. This reduction in AF recurrence  
370 rate is due to the synergistic effect of the two treatments to reduce the number of wavefront-  
371 wavetail interactions, thereby lowering the rate of new wavefront generation and thus the  
372 number of active fibrillation waves.

## 373 **7 Sources of funding**

374 This work was supported by the Swiss National Supercomputing Centre (CSCS) under  
375 project ID s778 and by grants to US from the Netherlands Heart Foundation (CVON2014-09,  
376 RACE V: Reappraisal of Atrial Fibrillation: Interaction between hypercoagulability,  
377 Electrical remodelling, and Vascular Destabilisation in the Progression of AF), and the  
378 European Union (ERACoSysMED H2020 ERA-NET, Marie Skłodowska-Curie grant  
379 agreement No. 675351). Dr Conte is supported by the Swiss National Foundation (SNF)  
380 (Ambizione grant no PZ00P3\_180055 / 1).

## 381 **8 Conflict of interest**

382 Angelo Auricchio (AA) is a consultant to Boston Scientific, Backbeat, Biosense Webster,  
383 Cairdac, Corvia, Microport CRM, Philips, Radcliffe Publisher. He received speaker fee from  
384 Boston Scientific, Medtronic, and Microport. He participates in clinical trials sponsored by  
385 Boston Scientific, Medtronic, Philips. He has intellectual properties with Boston Scientific,  
386 Biosense Webster, and Microport CRM. Ulrich Schotten (US) received consultancy fees or  
387 honoraria from Johnson & Johnson, Roche Diagnostics, and Bayer Healthcare. US is co-  
388 founder and shareholder of YourRhythmics BV. He holds intellectual property with Roche  
389 and YourRhythmics BV. The other authors have nothing to declare.

390

391

- 393 [1] Rillig A, Lin T, Ouyang F, Heinz Kuck K, Richard Tilz R. Comparing  
394 Antiarrhythmic Drugs and Catheter Ablation for Treatment of Atrial Fibrillation. *J Atr*  
395 *Fibrillation* 2013; **6**: 861.
- 396 [2] Hakalahti A, Biancari F, Nielsen JC, Raatikainen MJ. Radiofrequency ablation vs.  
397 antiarrhythmic drug therapy as first line treatment of symptomatic atrial fibrillation:  
398 systematic review and meta-analysis. *Europace* 2015; **17**: 370-378.
- 399 [3] Vogler J, Willems S, Sultan A, Schreiber D, Luker J, Servatius H, et al. Pulmonary  
400 Vein Isolation Versus Defragmentation: The CHASE-AF Clinical Trial. *J Am Coll Cardiol*  
401 2015; **66**: 2743-2752.
- 402 [4] Kuck KH, Brugada J, Furnkranz A, Metzner A, Ouyang F, Chun KR, et al.  
403 Cryoballoon or Radiofrequency Ablation for Paroxysmal Atrial Fibrillation. *N Engl J Med*  
404 2016; **374**: 2235-2245.
- 405 [5] Kirchhof P, Camm AJ, Goette A, Brandes A, Eckardt L, Elvan A, et al. Early  
406 Rhythm-Control Therapy in Patients with Atrial Fibrillation. *N Engl J Med* 2020.
- 407 [6] Duytschaever M, Demolder A, Philips T, Sarkozy A, El Haddad M, Taghji P, et al.  
408 Pulmonary vein isolation With vs. without continued antiarrhythmic Drug treatment in  
409 subjects with Recurrent Atrial Fibrillation (POWDER AF): results from a multicentre  
410 randomized trial. *Eur Heart J* 2018; **39**: 1429-1437.
- 411 [7] Fenner MF, Carstensen H, Dalgas Nissen S, Melis Hesselkilde E, Scott Lunddahl C,  
412 Adler Hess Jensen M, et al. Effect of selective IK,ACh inhibition by XAF-1407 in an equine  
413 model of tachypacing-induced persistent atrial fibrillation. *Br J Pharmacol* 2020; **177**: 3778-  
414 3794.
- 415 [8] Gharaviri A, Bidar E, Potse M, Zeemering S, Verheule S, Pezzuto S, et al. Epicardial  
416 Fibrosis Explains Increased Endo-Epicardial Dissociation and Epicardial Breakthroughs in  
417 Human Atrial Fibrillation. *Front Physiol* 2020.
- 418 [9] Whitaker J, Rajani R, Chubb H, Gabrawi M, Varela M, Wright M, et al. The role of  
419 myocardial wall thickness in atrial arrhythmogenesis. *Europace* 2016; **18**: 1758-1772.
- 420 [10] Verheule S, Eckstein J, Linz D, Maesen B, Bidar E, Gharaviri A, et al. Role of endo-  
421 epicardial dissociation of electrical activity and transmural conduction in the development of  
422 persistent atrial fibrillation. *Prog Biophys Mol Biol* 2014; **115**: 173-185.
- 423 [11] Courtemanche M, Ramirez RJ, Nattel S. Ionic mechanisms underlying human atrial  
424 action potential properties: insights from a mathematical model. *Am J Physiol* 1998; **275**:  
425 H301-321.
- 426 [12] Gharaviri A, Verheule S, Eckstein J, Potse M, Kuklik P, Kuijpers NH, et al. How  
427 disruption of endo-epicardial electrical connections enhances endo-epicardial conduction  
428 during atrial fibrillation. *Europace* 2017; **19**: 308-318.
- 429 [13] Krause D, Potse M, Dickopf T, Krause R, Auricchio A, Prinzen F. Hybrid  
430 Parallelization of a Large-Scale Heart Model. In: Keller R, Kramer D and Weiss J-P, eds.  
431 *Facing the Multicore - Challenge II*. Springer Berlin Heidelberg 2012: 120-132.
- 432 [14] Dobrev D, Friedrich A, Voigt N, Jost N, Wettwer E, Christ T, et al. The G protein-  
433 gated potassium current I(K,ACh) is constitutively active in patients with chronic atrial  
434 fibrillation. *Circulation* 2005; **112**: 3697-3706.
- 435 [15] Dobrev D, Graf E, Wettwer E, Himmel HM, Hala O, Doerfel C, et al. Molecular basis  
436 of downregulation of G-protein-coupled inward rectifying K(+) current (I(K,ACh) in chronic  
437 human atrial fibrillation: decrease in GIRK4 mRNA correlates with reduced I(K,ACh) and  
438 muscarinic receptor-mediated shortening of action potentials. *Circulation* 2001; **104**: 2551-  
439 2557.

- 440 [16] Voigt N, Abu-Taha I, Heijman J, Dobrev D. Constitutive activity of the acetylcholine-  
441 activated potassium current  $I_{K,ACh}$  in cardiomyocytes. *Adv Pharmacol* 2014; **70**: 393-409.
- 442 [17] Spach MS, Dolber PC. Relating extracellular potentials and their derivatives to  
443 anisotropic propagation at a microscopic level in human cardiac muscle. Evidence for  
444 electrical uncoupling of side-to-side fiber connections with increasing age. *Circ Res* 1986;  
445 **58**: 356-371.
- 446 [18] Pezzuto S, Gharaviri A, Schotten U, Potse M, Conte G, Caputo ML, et al. Beat-to-  
447 beat P-wave morphological variability in patients with paroxysmal atrial fibrillation: an in  
448 silico study. *Europace* 2018; **20**: iii26-iii35.
- 449 [19] Santangeli P, Marchlinski FE. Techniques for the provocation, localization, and  
450 ablation of non-pulmonary vein triggers for atrial fibrillation. *Heart Rhythm* 2017; **14**: 1087-  
451 1096.
- 452 [20] Gharaviri A, Verheule S, Eckstein J, Potse M, Kuijpers NH, Schotten U. A computer  
453 model of endo-epicardial electrical dissociation and transmural conduction during atrial  
454 fibrillation. *Europace* 2012; **14 Suppl 5**: v10-v16.
- 455 [21] Grandi E, Dobrev D, Heijman J. Computational modeling: What does it tell us about  
456 atrial fibrillation therapy? *Int J Cardiol* 2019; **287**: 155-161.
- 457 [22] Grandi E, Ripplinger CM. Antiarrhythmic mechanisms of beta blocker therapy.  
458 *Pharmacol Res* 2019; **146**: 104274.
- 459 [23] Rattanawong P, Kewcharoen J, K SS, Shen WK. Drug Therapy for Vagally-Mediated  
460 Atrial Fibrillation and Sympatho-Vagal Balance in the Genesis of Atrial Fibrillation: A  
461 Review of the Current Literature. *J Atr Fibrillation* 2020; **13**: 2410.
- 462 [24] Sanchez C, Bueno-Orovio A, Pueyo E, Rodriguez B. Atrial Fibrillation Dynamics and  
463 Ionic Block Effects in Six Heterogeneous Human 3D Virtual Atria with Distinct  
464 Repolarization Dynamics. *Front Bioeng Biotechnol* 2017; **5**: 29.
- 465 [25] Rotter M, Dang L, Jacquemet V, Virag N, Kappenberger L, Haissaguerre M. Impact  
466 of varying ablation patterns in a simulation model of persistent atrial fibrillation. *Pacing Clin*  
467 *Electrophysiol* 2007; **30**: 314-321.
- 468 [26] Grandi E, Maleckar MM. Anti-arrhythmic strategies for atrial fibrillation: The role of  
469 computational modeling in discovery, development, and optimization. *Pharmacol Ther* 2016;  
470 **168**: 126-142.
- 471 [27] McDowell KS, Zahid S, Vadakkumpadan F, Blauer J, MacLeod RS, Trayanova NA.  
472 Virtual electrophysiological study of atrial fibrillation in fibrotic remodeling. *PLoS One*  
473 2015; **10**: e0117110.
- 474 [28] Verma A, Jiang CY, Betts TR, Chen J, Deisenhofer I, Mantovan R, et al. Approaches  
475 to catheter ablation for persistent atrial fibrillation. *N Engl J Med* 2015; **372**: 1812-1822.
- 476 [29] Boyle PM, Zahid S, Trayanova NA. Using personalized computer models to custom-  
477 tailor ablation procedures for atrial fibrillation patients: are we there yet? *Expert Rev*  
478 *Cardiovasc Ther* 2017; **15**: 339-341.
- 479 [30] Zahid S, Whyte KN, Schwarz EL, Blake RC, 3rd, Boyle PM, Chrispin J, et al.  
480 Feasibility of using patient-specific models and the "minimum cut" algorithm to predict  
481 optimal ablation targets for left atrial flutter. *Heart Rhythm* 2016; **13**: 1687-1698.
- 482 [31] Ali RL, Hakim JB, Boyle PM, Zahid S, Sivasambu B, Marine JE, et al.  
483 Arrhythmogenic propensity of the fibrotic substrate after atrial fibrillation ablation: a  
484 longitudinal study using magnetic resonance imaging-based atrial models. *Cardiovasc Res*  
485 2019; **115**: 1757-1765.

486

487

488 **Figure 1:** A) Simulated action potentials during AF episodes in control and  $I_K$  blockade  
489 simulations. Examples of simulated ECG in B) control and C)  $I_K$  blockade simulation.

490 **Figure 2:** Consecutive snapshots of conduction patterns and corresponding ECG leads (II,  
491 V1, and V3) in  $I_K$  blockade, PVI, and  $I_K$  blockade combined with PVI simulations with severe  
492 fibrosis. Black star indicates the stimulation point.

493 **Figure 3:** Atrial fibrillation (AF) and atrial flutter (AFL) initiation likelihood in control (no  
494  $I_K$  blockade and no PVI), PVI, and PVI +  $I_K$  blockade with different degrees of fibrosis.

495 **Figure 4:** Electrophysiological parameters. A) Examples of wave life spans in control,  $I_K$   
496 blockade, PVI, and PVI +  $I_K$  blockade simulations with severe fibrosis (the slope of the fitted  
497 red line indicates the wave generation rate). B) Average number of waves per cycle. C)  
498 Average wave sizes per cycle. D) Wave generation rate. E) Wave lifespan median.

499

500 **Table 1.** Atrial fibrillation cycle length (AFCL) and Excitable gap (EG) in simulation groups  
 501 with different degrees of fibrosis.

Simulation Groups Fibrosis		Control	I <sub>K</sub> blockade	PVI	PVI + I <sub>K</sub> blockade	P Value
without	AFCL (ms)	147.12 ±15	210.52* ±14	187.12*±13	202.12* ±15	*P < 0.05
	EG (ms)	55.28 ± 4.3	59.2 ± 3.1	58.2 ± 2.9	57.9 ± 4.2	P > 0.05
moderate	AFCL (ms)	152.28 ±18	224.06* ±16	192.28*±14	204.06*±16	* P < 0.05
	EG (ms)	53.78 ± 3.1	58.77 ± 4.2	57.77 ± 3.3	57.77 ± 3.6	P > 0.05
severe	AFCL (ms)	197.13 ±12	229.12* ±17	228.44*±11	219.12*±13	* P < 0.05
	EG (ms)	54.64 ± 2.9	59.6 ± 3.8	57.6 ± 3.8	57.6 ± 3.1	P > 0.05

502

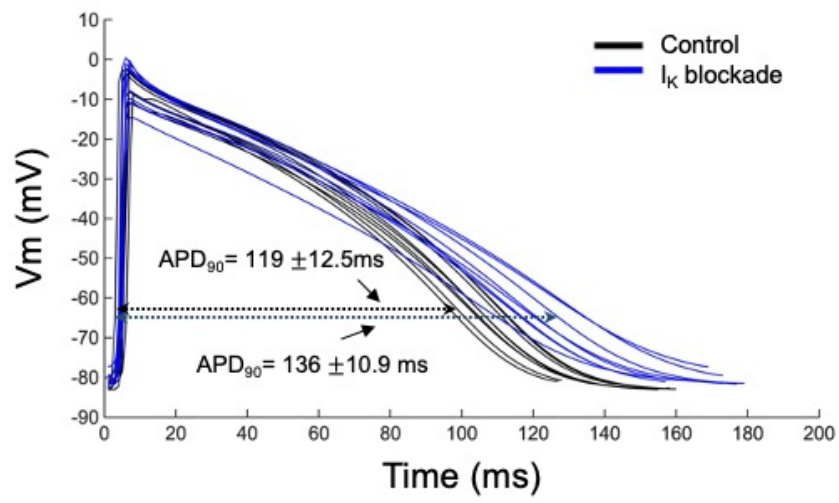
503

504

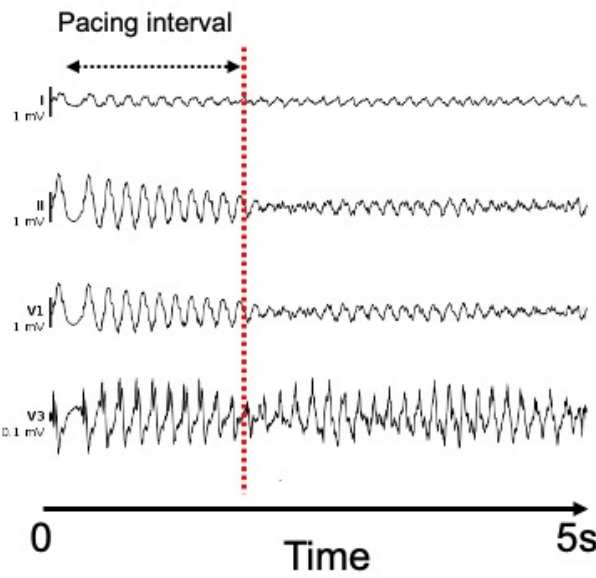
505

Figure 1

A



B



C

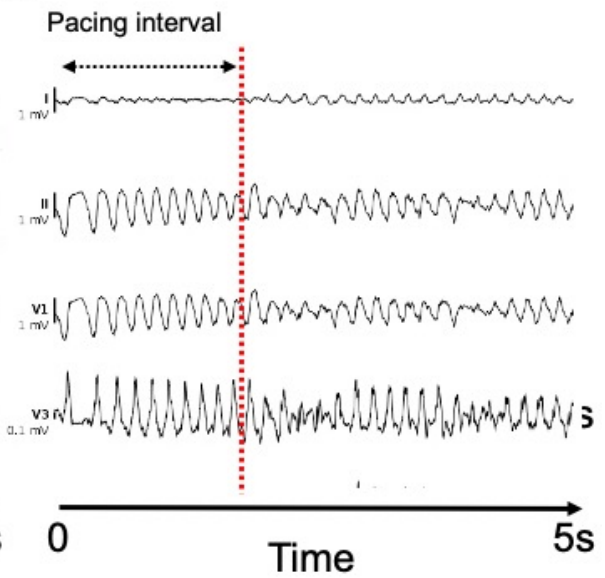


Figure 2

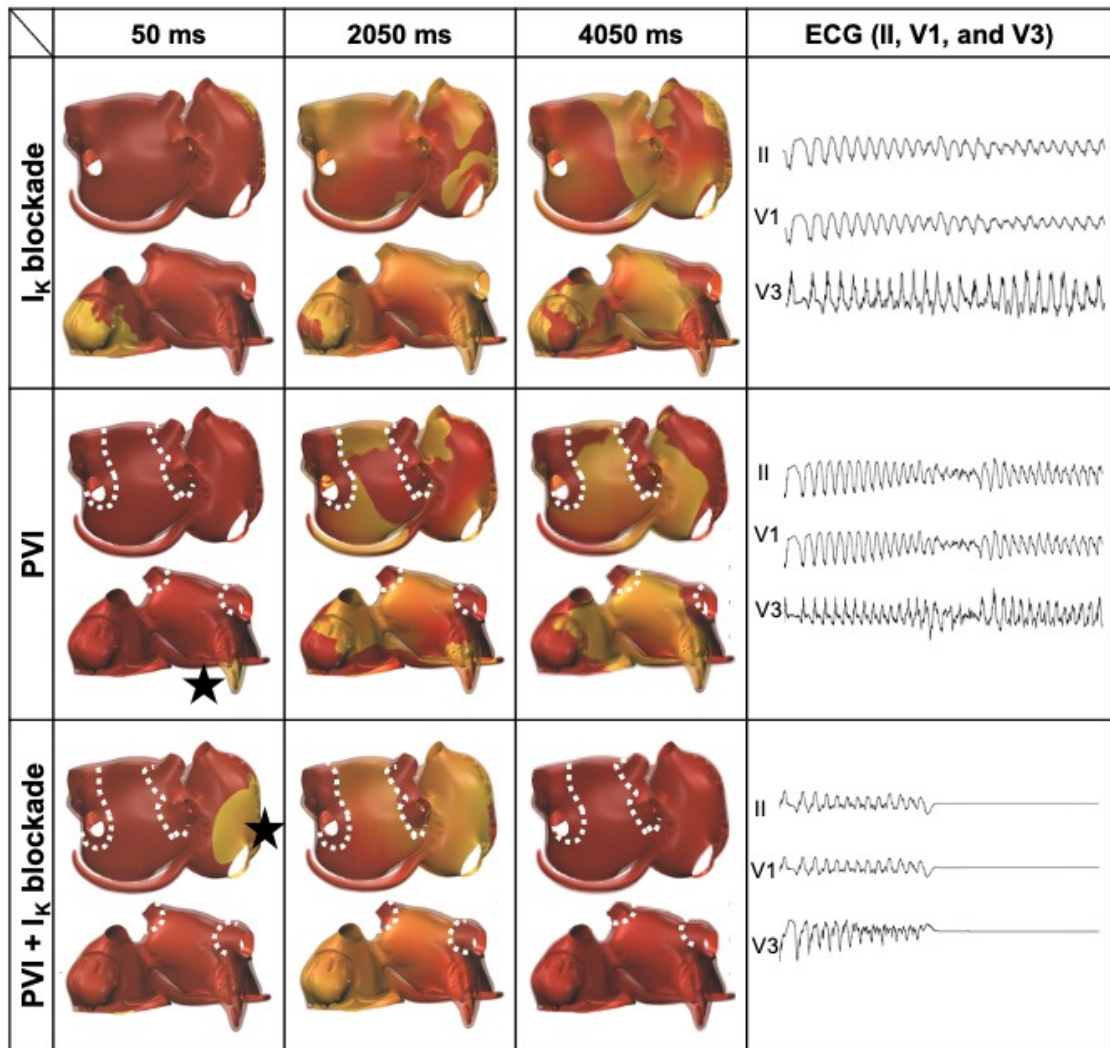


Figure 3

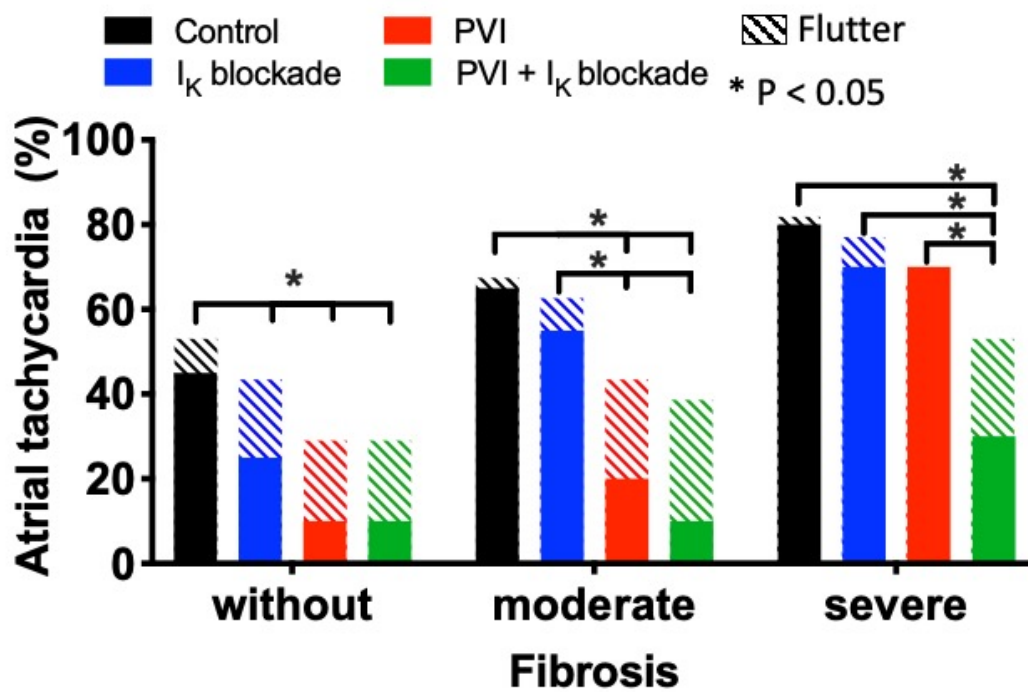


Figure 4

